



Hydrogenation of carbon dioxide to synthetic natural gas: impact of catalyst bed arrangement

二氧化碳加氢合成天然气：催化剂床安排之影响

Andreas Martin*, Daniel Türks, Hesham Mena, Udo Armbruster

Leibniz Institute for Catalysis, 18059 Rostock, Germany

andreas.martin@catalysis.de

Accepted for publication on 3rd December 2015

Abstract – Hydrogenation of carbon dioxide to synthetic natural gas (SNG) might be a future facet of energy storage solutions. This reaction can be run heterogeneously catalyzed at moderate pressure, it proceeds with high carbon dioxide conversions and extremely good SNG selectivity but it is highly exothermic. It can be operated at large scale in different reactor types but also in small units using simple tube reactors for decentralized solutions to turn excess electric power into storable SNG via intermediate hydrogen. In this paper, we describe the impact of catalyst bed arrangement on reaction heat distribution over the reactor as the basis for further simulations to receive the highest yield and productivity.

Keywords – carbon dioxide, synthetic natural gas, methanation, catalysis.

I. INTRODUCTION

Till date, the energy and chemical industries bases are mainly focused on the use of crude oil, natural gas and coal, in general. Only a minor part of other resources is applied in the energy sector such as nuclear and hydroelectric power, wind, geothermal energy, solar radiation and biomass. The global chemical industries used about 750 million tons of crude oil equivalents in 2012. Two third of this amount is covered by crude oil itself, 13% stems from natural gas and only 4% from coal [1]. Remarkably, 15% belongs to biomass feedstock (e.g. oils and fats, sugars, starch, cellulose etc.). However, sustainable and “green” resources have to be fixed for future applications because the fossil resources are finite. This scenario also applies to the energy sector. Time is short and the maximum of crude oil production, so called “peak oil”, is expected soon. Therefore, our world is presently facing a feedstock change with respect to energy production and chemical industry, too [e.g. 2, 3].

One of these alternatives might be the manufacture of biogas from different biomass sources, e.g. via fermentation. In general, biogas contains carbon dioxide and methane (50-70 vol% of CH₄ in dependence on feed); in addition, some impurities like hydrogen, hydrogen sulfide, nitrogen, ammonia and water vapor are present. World biogas production rapidly increased in recent years. More than 14,000 biogas plants (>7,500 MW power generation) existed in Europe by the end of 2013. Germany, Austria, UK and Sweden are leading in terms of its utilization for various applications (e.g. electricity, heat or fuels). Germany is Europe's biggest biogas producer and world leader in biogas technology. Roughly 8,000 plants (in 2014) are generating 3,859 MW of power with an annual turnover of ~7.9 billion €. However, the fraction of CH₄ produced from fermentation of renewables has only reached 3% of the total German CH₄ consumption [1-3]. Beside energetic usage of the biogas methane fraction by combustion, biogas also can be seen as a future raw material for chemical syntheses. A known example of combined use of both CH₄ and CO₂ is the “dry reforming” reaction to produce syngas (CO, H₂) [e.g. 4]. Another suitable option is the direct conversion of methane into formaldehyde or methanol via selective oxidation [e.g. 5, 6]. Moreover, the carbon dioxide portion might serve as feedstock for the manufacture of substitute or synthetic natural gas (SNG) by hydrogenation [e.g. 7].

At present, an increasing amount of electric power is produced from wind parks, biogas and photovoltaic plants. However, these energies are subjected to temporal fluctuation due to weather conditions. Very often wind turbines have to be switched off not to overstress the power grid. Indeed, one of the emerging tasks in future energy supply is the effective storage of electric power. An often discussed storage option for such excess electrical energy would be the generation of “green” hydrogen by water electrolysis and its temporal

storage in already available infrastructures like the gas grid, underground caverns or high pressure and liquid hydrogen tanks. But only lower amounts in single-digit percentage range might be allowed in gas grid or caverns, otherwise liquid hydrogen needs costly equipment.

The chemical conversion of such “green” hydrogen and easily available carbon dioxide to SNG is known as Sabatier reaction [8, 9]. Thereby, CO₂ fraction in biogas could be upgraded to SNG, significantly increasing the productivity of a biogas plant. This long-serving reaction is carried out in industry for cleaning of hydrogen from steam reforming in the presence of hydrogenation catalysts to remove CO and CO₂ traces [e.g. 10]. The reaction is highly exothermic and controlled by chemical equilibrium, and therefore the process is run at ca. 250-400 °C mainly over Ni-containing catalysts. It benefits from increasing pressure and is very selective toward SNG. At higher temperature, other reactions like reversed water-gas shift reaction affect the methane yield. Noble metal proportions might increase the productivity. A nice overview on applied catalyst systems is given in [11].

Interestingly, this process is suited to convert even considerable amounts of carbon dioxide, which are accessible not only from biogas plants, but also from power plants or chemical industries. This offers a large-scale chemical storage option, as “green” hydrogen is temporarily bound to carbon (CO₂) and CO₂ can be recycled with little loss. Anyway, it will definitely not solve the global CO₂ problem.

Car manufacturer Audi’s new power-to-gas facility in Werlte (Lower-Saxony, Germany) [12] came into operation in mid-2013; it is a 6 MW_{el} plant (1.5 million normal m³ per annum) connected to a biogas plant. Clariant has supplied the methanation catalyst [13]. The world’s largest SNG plant went on-stream last year (1.4 billion normal m³ per annum) in Yining/China with catalysts and process technology from Haldor Topsoe [14].

As mentioned above, the Sabatier reaction is highly exothermic.



However, this is not a problem in conventional application where carbon oxide traces have to be removed from gas streams by hydrogenation, but in case of selective SNG synthesis, exothermicity might cause heat transfer problems and even thermal runaway of the reactor. As a first consequence, the chemical equilibrium may be shifted away from optimum conditions. Own experiments have already shown the formation of hot-spots up to 15 K at the top of the catalyst bed [7]. Kienberger and Karl reported on the conversion of a CO/CO₂ and H₂ feed stemming from biomass gasification showing a reaction temperature in the hot-spot zone of 460 °C and a gas outlet temperature of 270 °C [15]. Therefore, different reactor concepts are in operation such as cascades of fixed bed reactors with limited conversion, wall-cooled fixed bed reactors, fluidized bed reactors or slurry bubble reactors [16]. Brooks et al. recently offered a concept of SNG synthesis using microchannel reactors to effectively

remove generated heat from the reactor [17]. Anyway, hot-spots may also lead to catalyst or reactor material damage and have to be avoided. Therefore, the aim of the present work was directed to collect data on heat distribution over the catalyst bed of a tube reactor at greatest possible SNG productivity for further simulation of catalyst bed arrangement.

II. REACTOR CONCEPT AND CATALYST

The catalytic tests were carried out with a lab set-up containing several mass flow controllers to meter feed gases, a suitable tube reactor, and a pressure transducer to measure reaction pressure, an automated pressure release valve and an on line-gas chromatograph unit for quick analysis of the feed and product stream. Details can be found elsewhere [7]. Two different stainless steel tube reactors (a) L = 276 mm, ID = 7.6 mm, V = 12.5 cm³ and (b) L = 1000 mm, ID = 24.8 mm, V = 483 cm³ with heating jacket (electrical heater and oil bath, respectively) were used. Both the reactors contain a guiding tube for a moveable thermocouple to stepwise record the catalyst bed temperature. Most of the runs reported here were carried out under the following conditions: T = 250-400 °C (set temperature), p = 10 bar, GHSV = 6000-12000 h⁻¹ (referred to standard reference conditions), CO₂: H₂ = 1: 4. In addition, nitrogen (10 vol%) was always fed as internal standard to evaluate volume contraction.

Carbon dioxide conversion (X_{CO₂}) and methane (S_{CH₄}) selectivity (S_{CH₄}) were determined from mole streams (n) and number of carbon atoms (z) as follows:

$$X_{\text{CO}_2} = \frac{\dot{n}_{\text{CO}_2(\text{in})} - \dot{n}_{\text{CO}_2(\text{out})}}{\dot{n}_{\text{CO}_2(\text{in})}} \times 100 \%$$

$$S_{\text{CH}_4} = \frac{\dot{n}_{\text{CH}_4}}{\dot{n}_{\text{CO}_2(\text{in})} - \dot{n}_{\text{CO}_2(\text{out})}} \times \frac{z_{\text{CH}_4}}{z_{\text{CO}_2}} \times 100 \%$$

First tests on temperature and pressure dependency were mainly carried out over a homemade 5 wt% Ni/ZrO₂ catalyst [7, 18]. An industrially available Ni-containing catalyst (18 wt% Ni on alumina (original size: 2.5×3-5 mm extrudates), denoted as 18Ni) was used for all catalytic runs with respect to temperature profile recording. The catalyst particles were crushed and sieved, and the fraction of 500-800 μm was used for all runs. Quartz split of the same size was used for catalyst dilution. Before catalytic tests, the catalyst was in-situ activated in hydrogen.

III. CATALYST TEST RUNS

Previous studies using monometallic Ni-, Ru and bimetallic NiRu-containing catalysts in a larger temperature and pressure

window have shown that the best results with respect to carbon dioxide conversion and SNG selectivity were received at 10 bar and 325-350 °C. In particular, an increased reaction pressure is beneficial to suppress CO and ethane formation. Observed carbon dioxide conversion always is close to the thermodynamic equilibrium [cf. 7, 18] and SNG selectivity is above 99.9%. There are two different mechanistic routes under discussion: i) the direct hydrogenation of CO₂ to methane without the formation of CO as intermediate and ii) the conversion of CO₂ to CO (reverse water gas shift reaction), followed by a methanation reaction according to the mechanism as of CO methanation [e.g. 19, 20]. CO forms an adsorbed carbon species (C_a) on the catalyst surface and is subsequently hydrogenated to methane by surface hydrogen [e.g. 19, 20]. In other words, the methanation mechanism might be characterized by carbon formation and carbon methanation. However, adsorbed CO may react at low temperatures to hydrocarbons via the Fischer-Tropsch reaction (conversion of CO and H₂) [e.g. 21]. Indeed, our previous runs always revealed some ethane formation (<1%) at temperatures up to 325 °C [7]. However, ethane might also be formed at higher temperatures but it is easily converted to methane in surplus of hydrogen by hydrogenolysis [22]. Table 1 gives a short summary on the results with 5 wt% Ni/ZrO₂ catalyst received so far.

TABLE 1, CARBON DIOXIDE CONVERSION AND SNG SELECTIVITY IN 300-400 °C TEMPERATURE RANGE AT DIFFERENT REACTION PRESSURE

T (°C)	300	325	350	375	400
X _{CO2} ^a	98.5	97.7	96.5	95.5	94.0
X _{CO2} ^b	19.5	38.5	54.3	66.0	71.1
X _{CO2} ^c	96.7	96.8	95.9	94.6	93.2
S _{SNG} ^b	99.0	99.5	99.6	99.2	98.9
S _{SNG} ^c	99.8	99.9	100	99.9	99.9

5wt% Ni/ZrO₂ catalyst, GHSV = 6000 h⁻¹, CO₂: H₂: N₂ = 1: 4: 5, ^a CO₂ equilibrium conversion (at 1 bar), ^b CO₂ conversion and SNG selectivity at 1 bar, ^c CO₂ conversion and SNG selectivity at 10 bar

As already mentioned, catalytic test runs at higher SNG productivity due to increased space velocity and reduced inert gas proportion and/or higher catalyst proportion showed pronounced hot-spots in the topmost part of the catalyst bed. As a crucial requirement for up-scaling trials, knowledge on prevention of hot-spot at high catalyst load is indispensable. Therefore, several tests on the arrangement of the catalyst bed at increased space velocity as well as decreased inert gas dilution (10 vol% N₂) were carried out using an industrially available catalyst.

IV. TEMPERATURE PROFILES

Figure 1 schematically depicts the used lab tube reactor and the position of quartz split layers above and below the catalyst bed each separated by quartz wool. The right-hand scale (in cm) shows the length of the guiding tube for a thermocouple which allows temperature measurement along the catalytic bed. Length data in the figures below refer to those given here.

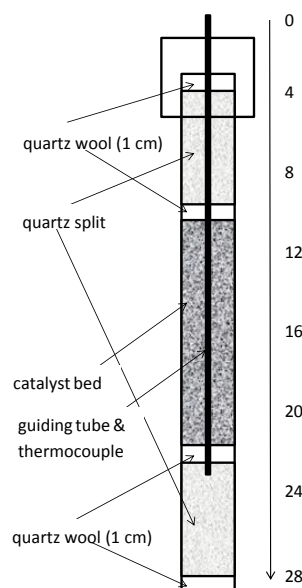


Fig.1, Schematic image of the used lab reactor and arrangement of catalyst bed (right-hand numbers are in cm).

First tests were carried out keeping the GHSV constant (ca. 6000 h⁻¹) while the amount of catalyst and feed gas were increased proportionally in order to get a higher total SNG yield. The catalyst bed consisted of a 5 ml grain mixture containing 1 ml (run A), 2.5 ml (run B) and 4 ml (run C) of 18Ni catalyst diluted with quartz, i.e. 4 ml (A), 2.5 ml (B) and 1 ml (C). The feed gas flow was equivalently increased to keep GHSV constant: 6 l/h (A), 15 l/h (B) and 26.4 l/h (C). Highest SNG yields were observed at 325 °C (A), 300 °C (B) and 290 °C (C) set point temperature, however, one can see that hot-spot temperatures are significantly increased, i.e. they reached 325 °C, 336 °C and 358 °C, respectively. Higher set point temperatures resulted in decreasing X_{CO2} due to equilibrium restrictions, in particular for runs A and B, however, selectivity to SNG was quite stable reaching values >99.9%. Data for run C were only be collected up to 290 °C because the hot-spot climbed up to >70 K. Table 2 summarizes these data.

TABLE 2, CARBON DIOXIDE CONVERSION AND SELECTIVITY TO SNG DURING TEST RUNS WITH DECREASING CATALYST DILUTION

T (°C)	270	280	290	300	325	350	375
A X _{CO2}				96.5	96.9	96.1	95.1
A S _{SNG}				99.9	99.9	99.9	99.9
B X _{CO2}				97.3	96.8	96.5	95.4
B S _{SNG}				99.9	99.9	99.9	99.9
C X _{CO2}	96.5	96.7	97.4				
C S _{SNG}	99.9	99.9	99.9				
A hot-spot				300	325	351	378
B hot-spot				336	361	384	406
C hot-spot	334	347	358				

GHSV = ca. 6000 h⁻¹, CO₂: H₂: N₂ = 1.8: 7.2: 1, run A: cat: quartz = 1: 4, 6 l/h feed, run B: cat: quartz = 1: 1, 15 l/h feed, run C: cat: quartz = 4: 1, 26.4 l/h feed, catalyst: 18Ni

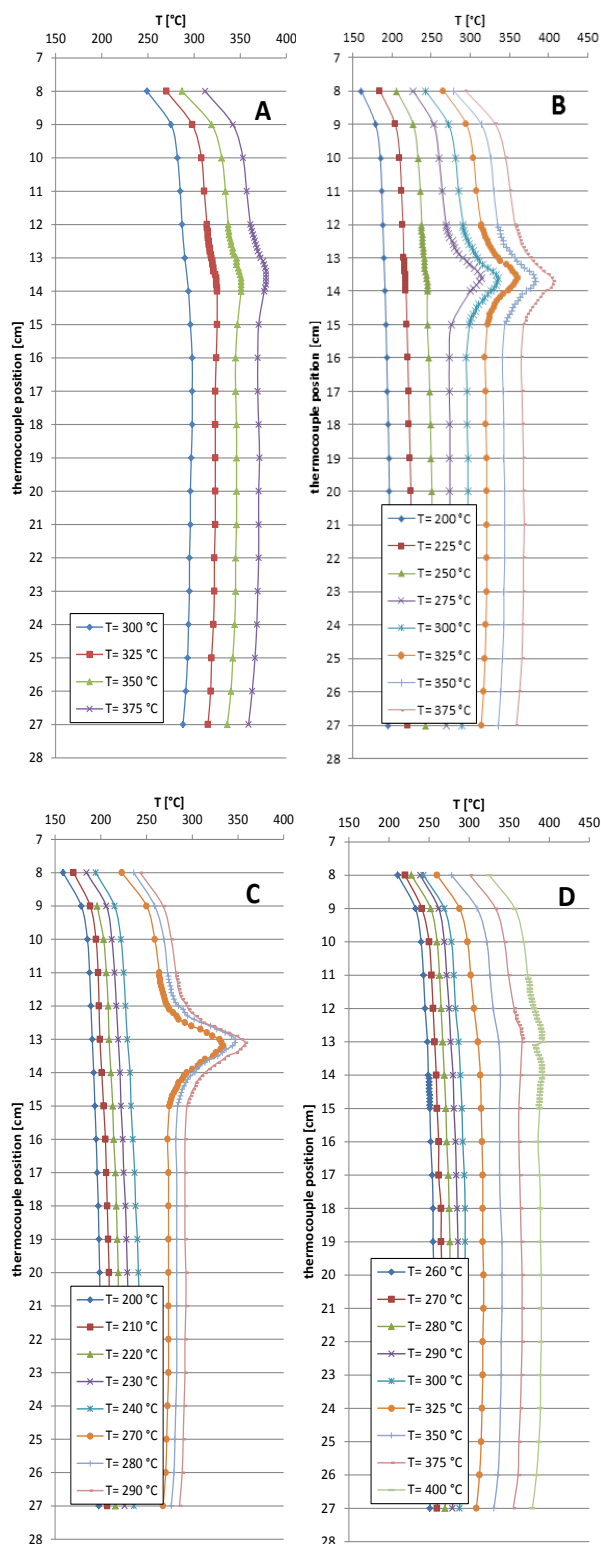


Fig.2, Temperature profiles of carbon dioxide hydrogenation runs (CO₂: H₂: N₂ = 1.8: 7.2: 1; run A: cat (1 ml): quartz = 1: 4, 6 l/h feed, 6000 h⁻¹; run B: cat (2.5 ml): quartz = 1: 1, 15 l/h feed, 6000 h⁻¹; run C: cat (4 ml): quartz = 4: 1, 26.4 l/h feed, 6000 h⁻¹; run D: cat (0.5 ml): quartz = 1: 9, 6 l/h feed, 12000 h⁻¹; catalyst: 18Ni).

The SNG productivity grew from 1.1 l_{SNG}/h (A) and 2.6 l_{SNG}/h (B) to 4.6 l_{SNG}/h (C) by increasing catalyst amount at constant space velocity, but a significantly elevated hot-spot temperature was the consequence. Therefore, the conversions were comparable at even less set point temperatures because the reaction temperatures in the hot-spot region were similar. Figure 2 shows the related temperature profiles and it is clear that the hot-spot appearance is very narrow but significant. Taking these results into account, further catalyst dilution combined with increased space velocity should lead to raised productivity at more equal temperature distribution over the whole bed.

Therefore, a further test (run E) with increased dilution of catalyst: diluent = 1: 9, i.e. 0.5 ml catalyst at increased GHSV (12000 h⁻¹) was carried out. It revealed similar carbon dioxide conversion and selectivity to SNG, but highest X_{CO₂} = 96.6% and S_{SNG} = 99.9% were observed at 350 °C. The SNG productivity in this run was close to 2.1 l_{SNG}/h. Interestingly, more or less no distinct hot-spot was observed as shown below (see Fig. 2). This illustrates the beneficial effect of improved temperature control on the chemical equilibrium.

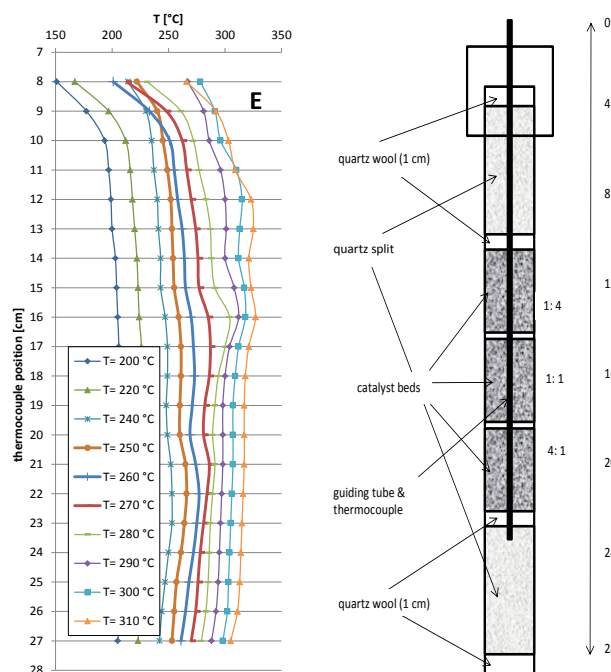


Fig.3, Temperature profile of carbon dioxide hydrogenation over structured catalyst bed (CO₂: H₂: N₂ = 1.8: 7.2: 1, GHSV = ca. 6000 h⁻¹, 13.5 l/h feed, three catalyst zones (1.7 ml each) catalyst: quartz split diluent ratio was varied top-down from 1: 4, 1: 1 to 4: 1, catalyst: 18Ni).

As a consequence of these first test runs, the diluted catalyst bed was divided into three parts of ca. 1.7 ml each (again 5 ml in total) as shown in Figure 3. The catalyst: quartz diluent ratio was varied top-down from 1: 4 to 1: 1 and 4: 1. The three zones were separated by small quartz wool layers of ca. 5 mm. In total, a catalyst: diluent ratio of 1: 1 (as in run B) was applied

but the above described structure of the bed should lead to altered hot-spot behavior. The hydrogenation run E was carried out at 6000 h⁻¹ and 13.5 l/h feed gas (CO₂: H₂: N₂ = 1.8: 7.2: 1). A carbon dioxide conversion close to equilibrium was reached at ca. 300-310 °C set point temperature, i.e. X_{CO₂} = 97.5%. The reaction temperatures in the first two beds reached 318 °C and 325 °C, respectively. This means a hot-spot of 8 and 15 K, respectively, is observed at a set point temperature of 310 °C. The SNG productivity amounted to 2.4 l_{SNG}/h, i.e. the same value was obtained as seen for run B but hot-spot behavior dramatically changed and overall reaction temperature decreased significantly.

Based on these results further optimization aiming at increasing SNG productivity is on the way. In addition, first test runs were carried out using the large lab reactor (as a start, catalyst volume was ca. 15 ml separated in the same way to the above described run E but using four catalyst zones). The results show that a larger tube reactor can be operated at similar conditions up to space velocities of about 40000 h⁻¹. SNG productivity was increased to 50 l/h that relates to an electrical power of 500 W. Such tubes might be incorporated in a multitube reactor to further increase of productivity.

IV. CONCLUSION

SNG synthesis was carried out with a commercially available Ni-containing catalyst. The catalyst dilution impact was studied to avoid hot-spot formation and damage of catalyst or reactor. The results have shown that most of the heat of reaction is produced in the topmost 10% of the catalyst bed at the feed inlet. The resulting hot-spot can be significantly suppressed by catalyst bed dilution and additionally by structuring the bed without changing overall catalyst mass. Thus, the reactor can be operated at higher load resulting in higher productivity. Catalyst dilution at the feed inlet should be very high and decrease in top-down direction.

Acknowledgments

The authors would like to thank the Federal State of Mecklenburg-Western Pomerania and the EU Regional Fund (EFRE) for funding (Project V-630-S-152-2012/141).

REFERENCES

- 1 J. Fabri and W. Falter, „Zeit für einen Rohstoffwandel?“ *Nachrichten aus der Chemiewirtschaft*, pp. 19-22, April 2013.
- 2 G.A. Olah, A. Goepfert, and G.K. Surya Prakash, *Beyond Oil and Gas: The Methanol Economy*. Weinheim: Wiley-VCH, 2009.
- 3 M.J. Climent, A. Corma, and S. Iborra, “Conversion of biomass platform molecules into fuel additives and liquid hydrocarbon fuels”, *Green Chem.*, **16**, pp. 516-547, 2014.
- 4 A. Wahyu Budiman, S.-H. Song, T.-S. Chang, C.-H. Shin, and M.-J. Choi, “Dry Reforming of Methane Over Cobalt Catalysts: A Literature Review of Catalyst Development”, *Catal. Surv. Asia*, **16**, pp. 183-197, 2012.
- 5 H. Berndt, A. Martin, A. Brückner, E. Schreier, D. Müller, H. Kosslick, G.-U. Wolf, and B. Lücke, “Structure and Catalytic Properties of VO_x/MCM Materials for the Partial Oxidation of Methane to Formaldehyde”, *J. Catal.*, **191**, pp. 384-400, 2000.
- 6 C. Pirovano, E. Schönborn, S. Wohlrab, N. Kalevaru, and A. Martin, “On the performance of porous silica supported VO_x catalysts in the selective oxidation of methane”, *Catal. Today*, **192**, pp. 20-27, 2012.
- 7 F. Lange, U. Armbruster, and A. Martin, “Heterogeneously-catalyzed hydrogenation of carbon dioxide to methane over RuNi-bimetallic catalysts”, *Energy Technol.*, **3**, pp. 55-62, 2015.
- 8 P. Sabatier and J.B. Senderens, “Nouvelles synthèses du méthane”, *C.R. Acad. Sci.*, **134**, pp. 514-516, 1902.
- 9 P. Sabatier and J.B. Senderens, “Hydrogénation directe des oxydes du carbone en présence de divers métaux divisés”, *C.R. Acad. Sci.*, **134**, pp. 689-691, 1902.
- 10 J.K. Nørskov, T. Bligaard, B. Hvolbæk, F. Abild-Pedersen, I. Chorkendorff, and C.H. Christensen, “The nature of the active site in heterogeneous metal catalysis”, *Chem. Soc. Rev.*, **37**, pp. 2163-2171, 2008.
- 11 G. Garbarino, P. Riani, L. Magistri, and G. Busca, “A study of the methanation of carbon dioxide on Ni/Al₂O₃ catalysts at atmospheric pressure”, *Int. J. Hydrogen Energy*, **39**, pp. 11557-11565, 2014.
- 12 http://www.audi.de/de/brand/de/vorsprung_durch_technik/content/2013/08/energiewende-im-tank.html
- 13 <http://www.chemicals-technology.com/news/news-clarient-catalyst-audi-german-methanation-plant>
- 14 <http://www.topsoe.com/Press/News/2013/281013.aspx>.
- 15 T. Kienberger and J. Karl, *Substitute natural gas (SNG) – Stand der Technik, theoretische Grundlagen, Forschung am Institut für Wärmetechnik*, 11. Symposium Energieinnovation, 10.-12.02.2010, Graz, Austria
- 16 <http://www.netl.doe.gov/research/coal/energy-systems/gasification/gasifipedia/coal-to-sng>
- 17 K.P. Brooks, J. Hu, H. Zhu, and R.J. Kee, “Methanation of carbon dioxide by hydrogen reduction using the Sabatier process in microchannel reactors”, *Chem. Eng. Sci.*, **62**, pp. 1161-1170, 2007.
- 18 M. Schoder, U. Armbruster, and A. Martin, “Heterogen-katalysierte Hydrierung von CO₂ zu Methan unter erhöhten Drücken“, *Chem. Ing. Tech.*, **85**, pp. 344-352, 2013.
- 19 D.E. Peebles, D.W. Goodman, and J.M. White, “Methanation of carbon dioxide on nickel(100) and the effects of surface modifiers”, *J. Phys. Chem.*, **27**, pp. 4378-4387, 1983.
- 20 W. Wang and J. Gong, “Methanation of carbon dioxide: an overview”, *Front. Chem. Sci. Eng.*, **5**, pp. 2-10, 2011.
- 21 G.P. van der Laan and A.A.C.M. Beenackers, “Kinetics and Selectivity of the Fischer-Tropsch Synthesis: A Literature Review”, *Catal. Rev.-Sci. Eng.*, **41**, pp. 255-318, 1999.

- 22 J. Yang, W. Ma, D. Chen, A. Holmen, and B.H. Davis,
“Fischer-Tropsch synthesis: A review of the effect of CO
conversion on methane selectivity” *Appl. Catal. A:
General*, **470**, pp. 250-260, 2014.